THE JOURNAL OF BIOLOGICAL CHEMISTRY VOL. 287, NO. 18, pp. 15054–15065, April 27, 2012

Sorting Nexin 27 Interacts with Multidrug Resistance-associated Protein 4 (MRP4) and Mediates Internalization of MRP4*[S]

Received for publication, December 29, 2011, and in revised form, March 9, 2012 Published, JBC Papers in Press, March 12, 2012, DOI 10.1074/jbc.M111.337931

Hisamitsu Hayashi[‡1], Sotaro Naoi[‡], Takayuki Nakagawa[‡], Toru Nishikawa[§], Hiroyuki Fukuda[¶], Shinobu Imajoh-Ohmi[¶], Ayano Kondo[‡], Kiyotaka Kubo[‡], Takashi Yabuki[‡], Asami Hattori[‡], Masakazu Hirouchi[‡], and Yuichi Sugiyama[‡2]

From the [‡]Laboratory of Molecular Pharmacokinetics, Department of Medical Pharmaceutics, Graduate School of Pharmaceutical Sciences, University of Tokyo, 7-3-1 Hongo, Bunkyo-ku, Tokyo 113-0033, Japan, the [§]Department of Psychiatry and Behavioral Sciences, Graduate School of Medical and Dental Sciences, Tokyo Medical and Dental University, 1-5-45, Yushima, Bunkyo-ku, Tokyo 113-8519, Japan, and [¶]Institute of Medical Science, University of Tokyo, 4-6-1 Shirokanedai, Minato-ku, Tokyo 108-8639, Japan

Background: Little is known about the molecular mechanism regulating MRP4 expression on the cell surface.
Results: SNX27 physically associates with MRP4 through PDZ-PDZ interaction and accelerates MRP4 internalization.
Conclusion: SNX27 mediates MRP4 internalization and thereby negatively modulates the cell surface expression and transport function of MRP4.
Significance: This study provides insights into the mechanisms responsible for MRP4 internalization and SNX27 function.

Multidrug resistance-associated protein 4 (MRP4/ABCC4) makes a vital contribution to the bodily distribution of drugs and endogenous compounds because of its cellular efflux abilities. However, little is known about the mechanism regulating its cell surface expression. MRP4 has a PDZ-binding motif, which is a potential sequence that modulates the membrane expression of MRP4 via interaction with PDZ adaptor proteins. To investigate this possible relationship, we performed GST pull-down assays and subsequent analysis with matrix-assisted laser desorption/ionization-time of flight mass spectrometry. This method identified sorting nexin 27 (SNX27) as the interacting PDZ adaptor protein with a PDZ-binding motif of MRP4. Its interaction was confirmed by a coimmunoprecipitation study using HEK293 cells. Knockdown of SNX27 by siRNA in HEK293 cells raised MRP4 expression on the plasma membrane, increased the extrusion of 6-[^{14}C]mercaptopurine, an MRP4 substrate, and conferred resistance against 6-[^{14}C]mercaptopurine. Cell surface biotinylation studies indicated that the inhibition of MRP4 internalization was responsible for these results. Immunocytochemistry and cell surface biotinylation studies using COS-1 cells showed that SNX27 localized to both the early endosome and the plasma membrane. These data suggest that SNX27 interacts with MRP4 near the plasma membrane and promotes endocytosis of MRP4 and thereby negatively regulates its cell surface expression and transport function.

The transport of solutes across biological membranes is indispensable for living organisms, and a number of transporters are implicated in this process. The ATP-binding cassette (ABC)[3] transporter superfamily is the largest transporter gene family. The multidrug resistance-associated protein 4 (MRP4) is the fourth member of subfamily C of the ABC transporter superfamily. This transporter was initially identified as a homologue of MRP1 by screening databases of human expressed sequence tags (1). Subsequent *in vitro* studies demonstrated the broad substrate specificity of MRP4, which includes cAMP, cGMP, GSH, and glucuronide conjugates (2–4). *In vivo* studies using MRP4-deficient mice have shown the vital contribution of MRP4 to the bodily distribution of these substrates (5–7). Loss of function of MRP4 in mice induces hematopoietic toxicity because of the accumulation of active metabolites of purine analogues in their myelopoietic cells (6) and tends to cause cystic fibrosis transmembrane conductance regulator (CFTR)-mediated secretory diarrhea through the disrupted regulation of cAMP concentration in the limited compartment (7). Thus, the physiological function of MRP4 is becoming clearer, although less is known about the regulation of its cell surface expression through posttranslational mechanisms.

MRP4 comprises 12 putative membrane-spanning domains and two ATP-binding motifs and contains a consensus class I PDZ-binding motif (PDZ-bm) at the C-terminal end (ETAL; $X(S/T)X\phi$, where X represents an unspecified residue and ϕ is a hydrophobic residue) (1, 8). The PDZ-bm interacts with pro-

* This study was supported by the Program for Promotion of Fundamental Studies in Health Sciences of the National Institute of Biomedical Innovation and Grant-in-Aid for Young Scientists (B) 23790175.
[S] This article contains supplemental Fig. 1.
[1] To whom correspondence may be addressed. Tel.: 81-3-5841-4773; Fax: 81-3-5841-4766; E-mail: hayapi@mol.f.u-tokyo.ac.jp.
[2] To whom correspondence may be addressed. Tel.: 81-3-5841-4770; Fax: 81-3-5841-4766; E-mail: sugiyama@mol.f.u-tokyo.ac.jp.

[3] The abbreviations used are: ABC, ATP-binding cassette; PDZ-bm, PDZ-binding motif; SNX, sorting nexin; 6MP, 6-mercaptopurine; CFTR, cystic fibrosis transmembrane conductance regulator; 5-HT$_{4(a)}$R, 5-hydroxytriptamine type-4(a) receptor; Kir3 channel, G protein-gated potassium channel; NR2C, *N*-methyl-D-aspartate receptor 2C; β2AR, β2-adrenoreceptor; 6TG, 6-thioguanine; KH, Krebs-Henseleit; Tfn, transferrin; AP2, AP2 adaptor complex; sulfo-NHS-SS-biotin, sulfosuccinimidyl 2-(biotinamido)-ethyl-1,3-dithiopropionate; Alexa594, Alexa Fluor 594-labeled Tfn.

teins containing a PDZ domain through a protein-protein interaction module, which is called PDZ-PDZ interaction, and mediates the correct sorting and tethering of membrane proteins to a specific subcellular localization by assembling the protein complex through this interaction (8, 9). It is conceivable that some PDZ domain-containing proteins interact with MRP4 via PDZ-PDZ interaction and modulate its expression on the plasma membrane. In the current study, we performed GST pull-down assays and subsequent analysis with matrix-assisted laser desorption/ionization-time of flight mass spectrometry (MALDI-TOF MS) and identified sorting nexin 27 (SNX27) as one of the partners that interacts with a PDZ-bm of MRP4.

SNX27 is a member of the SNX family of proteins, which are unified by the presence of a phox domain, a phospholipid-binding motif, and implicated in intracellular sorting and trafficking (10). SNX27 was originally identified in the rat neocortex as a developmentally regulated psychostimulant-inducible novel gene, which was designated as *mrt1* (methamphetamine-responsive transcript 1), having two splice forms (SNX27a (*mrt1a*) and SNX27b (*mrt1b*)) that vary only in their C-terminal ends (11). Among the SNX family, SNX27 is unique in that this protein is the only SNX member containing a PDZ domain (10, 11). SNX27 interacts with the PDZ-bm of a few membrane proteins through its PDZ domain and regulates their intracellular sorting (12–17). However, the function of SNX27 has not been characterized fully because the sorting process affected by SNX27 depends on the targeted proteins. SNX27 modulates the early endosomal trafficking of the 5-hydroxytryptamine type-4(a) receptor (5-$HT_{4(a)}$R), G protein-gated potassium (Kir3) channels, and *N*-methyl-D-aspartate receptor 2C (NR2C) (12, 13, 15). SNX27 also helps in the efficient recycling of β2-adrenoreceptor (β2AR) to the plasma membrane (14). Reports like these have generated interest in the association of SNX27 with the intracellular sorting of MRP4 in some processes and thereby in the regulation of the cell surface expression and transport function of MRP4.

Herein, we examined the effect of SNX27 suppression by siRNA in HEK293 cells on the cell surface expression of MRP4; sensitivity to 6-mercaptopurine (6MP) and 6-thioguanine (6TG), whose nucleotide metabolites are toxic MRP4 substrates; and endocytosis and recycling rates of MRP4. The cellular localization of SNX27 was explored in HEK293 and COS-1 cells. The data show that SNX27 interacts with MRP4 near the plasma membrane and promotes endocytosis of MRP4 and thereby negatively regulates its cell surface expression and transport function.

EXPERIMENTAL PROCEDURES

Materials—Antibodies against MRP4, lysosomal-associated membrane protein 1 (LAMP1), early endosome antigen 1 (EEA1), transferrin receptor, FLAG epitope (m2), hepatocyte growth factor-regulated tyrosine kinase substrate, and β-actin were purchased from Abcam (Cambridge, UK), BD Transduction Laboratories (San Diego, CA), BD Pharmingen (San Diego, CA), Invitrogen, Sigma-Aldrich, Novus Biologicals (Littleton, CO), and MP Biomedicals (Solon, OH), respectively. Antibodies against hypoxanthine phosphoribosyltransferase 1 (HPRT1) and thiopurine methyltransferase were obtained from Abnova (Taipei, Taiwan). Anti-SNX27 antibody, which recognizes both isoforms of SNX27 (11), was kindly provided by Dr. Toru Nishikawa (Tokyo Medical and Dental University, Tokyo, Japan). SNX27 expression was depleted selectively with siRNA targeting both isoforms of SNX27 (SNX27 siRNA) (sense, 5′-GGUUGGCAUGGACAGUACGTT-3′; antisense, 5′-CGUACUGUCCAUGCCAACCTT-3′) purchased from Ambion (Austin, TX). siRNA against firefly luciferase (control siRNA) was obtained from Dharmacon (Lafayette, CO). [^{14}C]6MP (51 mCi/mmol) was obtained from Moravek Biochemicals (Brea, CA). A human multiple-tissue blot (TB37-Set-I) was purchased from G-Biosciences (St. Louis, MO). All other chemicals were of analytical grade.

Construction of Plasmid Vectors—Human SNX27b (SNX27b) cDNA (NM_030918.5) was amplified by PCR with KOD Plus (Toyobo, Osaka, Japan) from cDNA of HEK293 cells and was subcloned into pcDNA3.1(+) (Neomycin) (Invitrogen). pcDNA3.1(+) (Neomycin) harboring human MRP4 (MRP4) cDNA (NM_005845) was constructed by subcloning of MRP4 cloned into pShuttle (Clontech, Palo Alto, CA) (5). cDNAs of human Rab4 (M28211), Rab5 (BC001267), Rab7 (BC013728), and Rab11 (AF000231) were generated by PCR from cDNA of HEK293 cells using the forward primers 5′-CACTCG AGCAATGTCCGAAACCTACG-3′ (Rab4), 5′-CACTCGAGACATGGCTAGTCGAGGCGCAAC-3′ (Rab5), 5′-GTCTCGAGGAAGGATGACCTCTAGGAAG-3′ (Rab7), and 5′-CACTCGAGCAATGGGCACCCGCGACGAC-3′ (Rab11) and the reverse primers 5′-GTGAATTCCTAACAACCACACTCCTGAGC-3′ (Rab4), 5′-GTGAATTCGGAAGCAGAAGACTATTCCAGC-3′ (Rab5), 5′-GTGAATTCCTCAGCAACTGCAGCTTTCTG-3′ (Rab7), and 5′-GTGAATTCCTTAGATGTTCTGACAGCAC-3′ (Rab11) and were subcloned into the EcoRI/XhoI restriction sites of pAcGFP-C1 (Clontech). cDNAs corresponding to the 100 amino acids in the C terminus of MRP4 (amino acid residues 1226–1325) (MRP4-C_{ter}) and the PDZ domain of SNX27 (SNX27 PDZ) (amino acid residues 43–134) were generated by PCR using the forward primers 5′-GGATCCTGCACCGTGCTAACCATTGCACAC-3′ (MRP4) and 5′-GGATCCCGCATCGTCAAGTCCG-3′ (SNX27) and the reverse primers 5′-GAATTCCAGTGCTGTCTCGAAAATAGTTAAGG-3′ (MRP4) and 5′-GAATTCCTAAGGTACAGATAACACTGTC-3′ (SNX27) and were subcloned into the BamHI/EcoRI restriction sites of the bacterial expression vector pGEX6P-2 (Amersham Biosciences). pBAsi-hU6 Pur DNA (Takara Bio Inc., Shiga, Japan) encoding shRNA against MRP4 (MRP4 shRNA) or firefly luciferase shRNA (control shRNA) was constructed by PCR involving empty pBAsi-hU6 Pur DNA vector with the following primers: 5′-CTTGTGGAAAGGACGAGGATCCGATGGTGCATGTGCAGGATCTCAAGAGAATCCTGCACATGCACCATCTTTTTTTCTAGAGTCGACCTGCAGGC-3′ and 5′-GCCTGCAGGTCGACTCTAGAAAAAAAGATGGTGCATGTGCAGGATTCTCTTGAGATCCTGCACATGCACCATCGGATCCTCGTCCTTTCCACAAG-3′ (MRP4 shRNA) and 5′-GCCTGCAGGTCGACTCTAGAAAAAAAACGTTACCGCGGAATACTTCGATCTCTTGAATGGCCAGCGTGCACATGCTGGATCCTCGTCCTTTCCACAAG-3′ and 5′-CTTGTGGAAAGGACGAGGATC-

CAGCATGTGCACGCTGGCCATTCAAGAGATCGAAGTATTCCGCGGTAACGTTTTTTTCTAGAGTCGACCTGCAGGC-3′ (control shRNA) (18). cDNAs of MRP4 with a FLAG epitope at the N terminus (FLAG-MRP4), FLAG-MRP4, and MRP4-C_{ter} lacking the last four amino acids of the C terminus (FLAG-MRP4Δ4 and MRP4-C_{ter}Δ4, respectively), were constructed using a QuikChange II XL site-directed mutagenesis kit (Stratagene, La Jolla, CA) according to the manufacturer's instructions (18). The sequences of the constructed vectors were confirmed using an ABI PRISM 3110 Genetic Analyzer (Applied Biosystems, Foster City, CA).

Cell Culture and Construction of MRP4 Knockdown Cells—HEK293, HeLa, COS-1, and HepG2 cells were cultured in Dulbecco's modified Eagle's medium (DMEM; Invitrogen) supplemented with 10% fetal bovine serum at 37 °C with 5% CO_2 and 95% humidity. pBAsi-hU6 Pur DNA encoding MRP4 shRNA or control shRNA was transfected into HEK293 cells with Fugene 6 (Roche Applied Science). After 48 h, transfected cells were selected with 1 μg/ml puromycin (Sigma-Aldrich). Several clones were isolated, and the expression of MRP4 was confirmed by Western blot analysis with anti-MRP4 antibody.

GST Fusion Protein Production and in Vitro Binding Assays—To construct the GST fusion protein with MRP4-C_{ter} (GST-MRP4-C_{ter}), MRP4-C_{ter}Δ4 (GST-MRP4-C_{ter}Δ4), and SNX27 PDZ (GST-SNX27 PDZ), the constructs of MRP4-C_{ter}, MRP4-C_{ter}Δ4, and SNX27 PDZ in the pGEX6P-2 vector were transformed into *Escherichia coli* BL21. A 5-ml aliquot of bacteria, grown overnight in LB medium containing 50 μg/ml ampicillin was transferred to 500 ml of 2× YT medium (1.6% tryptone, 1% yeast extract, 0.5% NaCl) containing 100 μg/ml ampicillin and cultured at 37 °C for an additional 3 h until the A_{600} reached 0.4. Protein expression was then induced by the addition of 0.1 mM isopropyl β-D-thiogalactoside and incubation overnight at 20 °C. After the induction, the bacteria were pelleted, washed, and resuspended in cold phosphate-buffered saline (PBS) containing a protease inhibitor mixture (Roche Applied Science) and 0.2 mM phenylmethylsulfonyl fluoride. Bacteria were solubilized with B-PER (bacterial protein extraction reagent) (Thermo Scientific, Rockford, IL). Cell debris was removed by centrifugation at 14,000 × *g* for 30 min at 4 °C, and the resulting bacterial lysate was either used immediately or stored at −80 °C until use. GST fusion proteins were purified by incubation with glutathione-agarose beads (Amersham Biosciences) for 2 h at 4 °C followed by washing with cold PBS. The amount of fusion protein eluted from the beads was quantified using the Lowry protein assay with bovine serum albumin (BSA) as the standard (19).

For *in vitro* binding assays, HepG2 cells were solubilized in lysis buffer (20 mM Tris-HCl, pH 7.5, 150 mM NaCl, 1 mM Na_2EDTA, 1 mM EGTA, 1% Triton X-100, 2.5 mM sodium pyrophosphate, 1 mM β-glycerophosphate, 1 mM Na_3VO_4, and 1 μg/ml leupeptin) containing a protease inhibitor mixture (Roche Applied Science) and 0.2 mM phenylmethylsulfonyl fluoride. The prepared lysate was then incubated with 50 μl of glutathione-agarose beads containing 50 μg of bound GST fusion protein for 2 h at 4 °C. After binding, the beads were washed three times in PBS containing 1% Triton X-100. Bound proteins were eluted with elution buffer (50 mM Tris-HCl, pH 8.0, 10 mM glutathione), separated by SDS-PAGE, and subjected to silver staining or Western blot analysis.

Protein Identification by Mass Spectrometry—Protein bands plus blank regions were excised from SDS-polyacrylamide gels visualized with silver staining and destained using a SilverQuest silver staining kit (Invitrogen) according to the manufacturer's instructions. After destaining, samples were subjected to in-gel digestion with a trypsin solution overnight at 37 °C. Supernatants were collected, washed with 0.1% trifluoroacetic acid (TFA), eluted with 50% acetonitrile solution containing 0.1% TFA, and analyzed by MALDI-TOF MS. A list of the determined peptide masses was subjected to mass fingerprinting using the Mascot software program (Matrix Science, London, UK), which was used to search the National Center for Biotechnology Information protein databases.

Immunoprecipitation—HEK293 cells were solubilized for 1 h at 4 °C in 1 ml of lysis buffer (10 mM Tris-HCl (pH 7.5), 150 mM NaCl, 1% Nonidet P-40, 5 mM $MgCl_2$, and 1 mM $CaCl_2$) and centrifuged at 12,000 × *g* for 10 min at 4 °C. The resultant supernatant was precleared by adding control IgG and 50 μl of protein G-Sepharose beads (Roche Applied Science). Three percent of each precleared lysate was preserved at −80 °C as the input specimen. The remaining precleared lysate was incubated with anti-FLAG or anti-SNX27 antibody for 2 h at 4 °C, after which 50 μl of protein G-Sepharose beads was added, and the lysate was incubated for 2 h at 4 °C. Immune complexes were precipitated, washed, and eluted as described previously (18, 20). The specimens were separated by SDS-PAGE and subjected to Western blot analysis.

Transport Study—The transport study was performed as reported previously (21). In brief, HEK293 cells expressing MRP4 shRNA (HEK-MRP4 shRNA) or control shRNA (HEK-control shRNA) were seeded onto 12-well plates coated with poly-L-lysine and poly-L-ornithine (Sigma-Aldrich) at a density of 4.0 × 10^5 cells/well and transfected with SNX27 siRNA or control siRNA using Lipofectamine RNAi Max (Invitrogen) according to the manufacturer's instructions. Forty-eight hours after siRNA transfection, the cells were washed once and preincubated with Krebs-Henseleit (KH) buffer (118 mM NaCl, 23.8 mM $NaHCO_3$, 4.83 mM KCl, 0.96 mM KH_2PO_4, 1.20 mM $MgSO_4$, 12.5 mM HEPES, 5.0 mM glucose, and 1.53 mM $CaCl_2$ adjusted to pH 7.4) at 37 °C for 15 min. The uptake and efflux assay was then initiated by adding KH buffer containing 5 μM [^{14}C]6MP. The uptake was terminated at a designated time by removing the incubation buffer and adding ice-cold KH buffer. The cells were washed three times with ice-cold KH buffer, solubilized in 0.2 N NaOH, and kept overnight at room temperature, and 0.4 N HCl was added. For the efflux assay, the cells were incubated for 2 h in KH buffer containing 5 μM [^{14}C]6MP, washed three times, and incubated with KH buffer at 37 °C. At the time points indicated, the incubation buffer was collected, and the cells were solubilized as described for the uptake assay. The radioactivity of the cell lysate and incubation buffer was measured in a liquid scintillation counter (LS 600SC, Beckman, Fullerton, CA) after mixing each sample with scintillation fluid (Clear-sol I; Nacalai Tesque, Kyoto, Japan) in a scintillation vial. The protein concentration of the cell lysate was measured by the Lowry method with BSA as the standard. The uptake value

was calculated as described previously (22). Efflux percentage was calculated by dividing the radioactivity in the incubation buffer at each time point by total radioactivity in the cell lysate and incubation buffer at that time point.

Cell Proliferation Assay—HEK-MRP4 shRNA and HEK-control shRNA cells were seeded into 96-well plates coated with poly-L-lysine and poly-L-ornithine at a density of 2.5×10^4 cells/well and transfected with SNX27 siRNA or control siRNA using Lipofectamine RNAi Max (Invitrogen) according to the manufacturer's instructions. The next day, various concentrations of 6MP, 6TG, and etoposide were added to the growth medium. After 96 h of growth in the presence of a drug, cell proliferation assays were performed using the CellTiter 96 cell proliferation assay (Promega, Madison, WI) according to the manufacturer's instructions.

Immunofluorescence—COS-1 cells were seeded onto glass coverslips (Matsunami Glass Ind. Ltd., Osaka, Japan) in 12-well plates at a density of 1.0×10^5 cells/well. In the experiments in which ectopically expressed Rab proteins were required, COS-1 cells were transfected with pAcGFP-C1 containing Rab4, Rab5, Rab7, or Rab11 using Lipofectamine 2000 (Invitrogen), harvested after 24 h of culture, and seeded as described above. Twenty-four hours after seeding, the cells were fixed in 4% paraformaldehyde, PBS for 10 min, permeabilized in 0.1% saponin, PBS for 10 min, blocked with 3% BSA, PBS for 30 min, and stained with anti-SNX27, anti-EEA1, and anti-LAMP1 antibodies for 2 h, followed by Alexa Fluor 488 donkey anti-mouse immunoglobulin G and Alexa Fluor 594 donkey anti-rabbit immunoglobulin G (Molecular Probes, Inc., Eugene, OR) for 1 h. These staining procedures were performed at room temperature. The cells were mounted onto glass slides with VECTASHIELD mounting medium (Vector Laboratories Inc., Burlingame, CA) and were visualized by confocal microscopy using a Leica TCS SP5 II laser-scanning confocal microscope (Leica, Solms, Germany).

Uptake of Alexa Fluor 594-labeled transferrin—COS-1 cells were seeded onto glass coverslips in 12-well plates at a density of 1.0×10^5 cells/well. Twenty-four hours after seeding, the cells were incubated in serum-free DMEM containing 0.2% BSA to deplete endogenous transferrin (Tfn) for 2 h. After incubation with Alexa Fluor 594-labeled Tfn (Alexa594 Tfn) (100 μg/ml) (Molecular Probes, Inc.) for the indicated time, surface-bound Alexa594 Tfn was removed by acid wash (50 mM glycine, 100 mM NaCl, pH 3.0). The cells were stained with anti-SNX27 antibody followed by Alexa Fluor 488 donkey anti-mouse immunoglobulin G according to the procedure described above and visualized by confocal microscopy using an LSM 510 apparatus (Carl Zeiss, Oberkochen, Germany).

Cell Surface Biotinylation and Determination of Rate of Degradation of Cell Surface Expressed Protein—HEK293 cells were seeded in 6-well plates coated with poly-L-lysine and poly-L-ornithine at a density of 8.0×10^5 cells/well. Forty-eight hours after seeding, cell surface biotinylation was performed using Sulfo-NHS-SS-biotin (Pierce) as described previously (23, 24). After cell solubilization, 5% of the biotinylated specimens were preserved to evaluate SNX27 expression in whole-cell lysates, and the remaining 95% of specimens were precipitated with streptavidin-agarose beads (Pierce) to prepare the cell surface fraction.

To examine the degradation rate of the cell surface-resident protein, HEK293 cells were seeded in 6-well plates coated with poly-L-lysine and poly-L-ornithine at a density of 8.0×10^5 cells/well and transfected with SNX27 siRNA or control siRNA using Lipofectamine RNAi Max according to the manufacturer's instructions. Cell surface biotinylation was performed after 48 h in culture. Biotinylated HEK293 cells were incubated for various periods at 37 °C before solubilization. The remaining biotinylated protein was then isolated with streptavidin-agarose beads as described previously (24, 25), separated by SDS-PAGE, and subjected to Western blot analysis.

Endocytosis and Recycling Assays—HEK293 cells were seeded in 6-well plates coated with poly-L-lysine and poly-L-ornithine at a density of 8.0×10^5 cells/well and transfected with SNX27 siRNA or control siRNA using Lipofectamine RNAi Max according to the manufacturer's instructions. An endocytosis assay was performed after 48 h in culture as described previously (24, 26). For recycling assays, the transfected cells were biotinylated after 48 h in culture and warmed to 37 °C for 15 min to load endocytic vesicles with biotinylated proteins. Cells were then cooled immediately to 4 °C and incubated with stripping buffer (50 mM Tris, 100 mM NaCl, 25 mM 2-mercaptoethanesulfonate, 25 mM dithiothreitol (pH 8.6)) at 4 °C to reduce the disulfide bonds between proteins labeled with sulfo-NHS-SS-biotin in the plasma membrane. Cells were then either lysed or warmed again to 37 °C for various periods to allow biotinylated MRP4 in the intracellular compartment to recycle to the plasma membrane. Cells were then cooled again to 4 °C, and the disulfide bonds in the proteins biotinylated with sulfo-NHS-SS-biotin remaining in the plasma membrane were reduced with stripping buffer. The recycling of internalized MRP4 was calculated as the difference between the amount of biotinylated MRP4 after the first and second incubation with stripping buffer.

Western Blot Analysis—Prepared specimens from each experiment were loaded into wells on a 7.5% SDS-PAGE plate with a 3.75% stacking gel and subjected to Western blot analysis as described previously (23, 25). Immunoreactivity was detected with an ECL Advance Western blotting detection kit (Amersham Biosciences). The intensity of the band indicating MRP4 was quantified using Multi Gauge software version 2.0 (Fujifilm, Tokyo, Japan).

Statistical Analysis—Experiments were repeated at least three times, and the data in the figures are presented as the means ± S.E. The significance of differences between two variables and between multiple variables was calculated at the 95% confidence level by Student's *t* test and one-way analysis of variance with Dunnett's test, respectively, using Prism software (GraphPad Software, Inc., La Jolla, CA).

RESULTS

Identification and Verification of PDZ-PDZ Interaction between MRP4 and SNX27—To identify the proteins that interact with the PDZ-bm of MRP4, GST-MRP4-C_{ter} and GST were generated and subjected to *in vitro* binding assays using lysates of

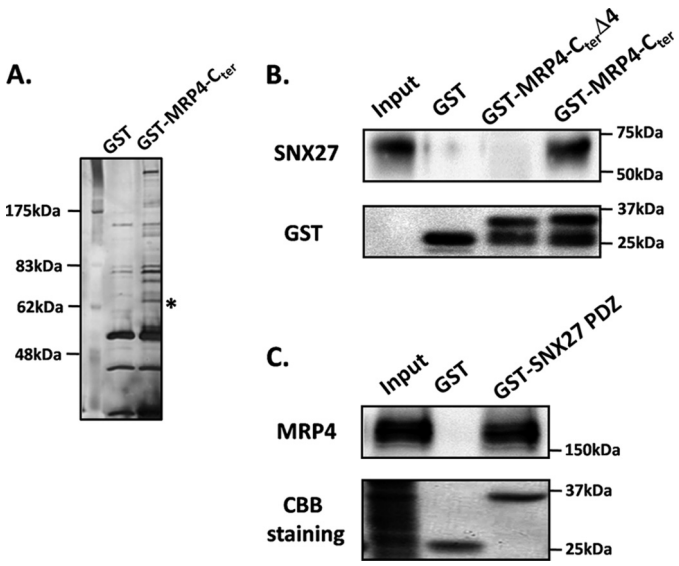

FIGURE 1. **Identification and verification of PDZ-PDZ interaction between MRP4 and SNX27.** GST, GST-MRP4-C_{ter} (residues 1226–1325), GST-MRP4-$C_{ter}\Delta4$ (residues 1226–1321), and GST-SNX27 PDZ (residues 43–134) (50 μg) were immobilized to 50 μl of glutathione-agarose beads and incubated with lysates from HepG2 cells for 2 h at 4 °C. The eluted samples were resolved on 7.5% SDS-PAGE and stained with silver (*A*) or subjected to Western blot analysis (*B* and *C*). A representative result from three independent experiments is shown. *, band analyzed by MALDI-TOF MS.

HepG2 cells, and the resultant specimens of the assays were resolved by SDS-PAGE (Fig. 1*A*). The specific protein band at ~62 kDa in SDS-PAGE (indicated by an *asterisk* in Fig. 1*A*) was analyzed by MALDI-TOF MS and was found to comprise SNX27. To verify that the interaction between MRP4 and SNX27 is through their PDZ-bm and PDZ-domains, GST-MRP4-C_{ter}, GST-MRP4-$C_{ter}\Delta4$, and GST-SNX27 PDZ were immobilized to glutathione-agarose beads and incubated with lysates from HepG2 cells. SNX27 was pulled down by GST-MRP4-C_{ter} but not by GST-MRP4-$C_{ter}\Delta4$ (Fig. 1*B*), and MRP4 was pulled down by GST-SNX27 PDZ but not by GST itself (Fig. 1*C*), indicating that the interaction of MRP4 and SNX27 occurs via PDZ-PDZ interaction. This interaction between MRP4 and SNX27 was confirmed in a study with lysates of HEK293 cells as well as HepG2 cells (data not shown).

GST-MRP4-C_{ter} and -MRP4-$C_{ter}\Delta4$ were detected as two bands (Fig. 1*B*). The upper bands around 37 kDa represent GST-MRP4-C_{ter} and -MRP4-$C_{ter}\Delta4$ themselves because these proteins were constructed with GST, a 26-kDa protein, with the amino acids corresponding to the C-terminal sequence of MRP4, a peptide of about 12 kDa, at the C-terminal end. By contrast, the lower bands seem to be degradation products of GST-MRP4-C_{ter} and -MRP4-$C_{ter}\Delta4$. Given that the bands were detected by a monoclonal antibody recognizing full-length GST, these products would have been derived from GST-MRP4-C_{ter} and -MRP4-$C_{ter}\Delta4$ cleaved at the part of the C-terminal sequence of MRP4.

Regulation of MRP4 Expression by SNX27—Western blot analysis using the human multiple-tissue panel showed that SNX27 is expressed ubiquitously in human tissues, including the kidney and brain (Fig. 2*A*), where MRP4 plays a pivotal role in drug disposition (5, 27) (Fig. 2*A*). The expression of SNX27 was also observed in mouse bone marrow (Fig. 2*B*), where MRP4 actively exports thiopurine nucleotides and prevents hematopoietic toxicity (6). The physiological interaction between MRP4 and SNX27 in bone marrow and kidney and in HEK293 cells was confirmed by coimmunoprecipitation and subsequent Western blot analysis using homogenates prepared from mouse bone marrow, kidney, and HEK293 cells (Fig. 2, *C* and *D*).

The functional association of SNX27 with MRP4 was next evaluated by observing the change in MRP4 expression by transfection of SNX27 siRNA targeting both isoforms of SNX27, SNX27a and SNX27b (Fig. 3*A*). HEK293, HeLa, and HepG2 cells were selected for this study because the endogenous expression of MRP4 and SNX27 and the interaction between these molecules were verified in these cell lines (Fig. 2*D*) (data not shown). The expression level of MRP4 was increased 2–3-fold by the suppression of SNX27 in all tested cells, and an approximately 4-fold increase in MRP4 was observed in the cell surface fraction of HEK293 cells (Fig. 3, *A* and *B*). Conversely, the overexpression of SNX27b in HEK293 cells decreased MRP4 expression by 2.5- and 3-fold in the cell lysates and cell surface fraction, respectively (Fig. 3, *C* and *D*). Taken together, these results indicate that SNX27 negatively regulates MRP4 expression in the cell lines cultured. No effect on the expression level of the Na^+/K^+-ATPase $\alpha1$ subunit was observed with the change in SNX27 expression (Fig. 3, *A*–*D*), suggesting that the SNX27-mediated regulation is specific for MRP4.

Effect of SNX27 Suppression on 6MP and 6TG Sensitivity—The change in MRP4 function by SNX27 suppression was examined by measuring the efflux of radioactivity from [^{14}C]6MP taken up into HEK293 cells because 6MP is intracellularly converted to thionucleoside monophosphates, which are toxic metabolites and good substrates of MRP4 (28). HEK-MRP4 shRNA and HEK-control shRNA were generated, and an approximately 5-fold lower MRP4 expression in HEK-MRP4 shRNA than in HEK-control shRNA was verified (Fig. 4*A*). Suppression of MRP4 function in HEK-MRP4 shRNA was confirmed by the lower efflux activity of [^{14}C]6MP and higher sensitivity to 6MP toxicity than those observed in HEK-control shRNA (Fig. 4*C* and Table 1). In contrast to the sensitivity assay, which produced a convincing result (Table 1), the efflux assay showed a modest difference between HEK-MRP4 shRNA and HEK-control shRNA (Fig. 4*C*). However, this can be explained by the fact that 6MP is metabolized to various compounds in HEK293 cells and is excreted predominantly in the form of MP riboside by equilibrative nucleoside transporters, not by MRP4, and that thio-IMP, a toxic metabolite of 6MP, is a good substrate of MRP4 (28).

The transfection of SNX27 siRNA significantly increased the [^{14}C]6MP efflux in HEK-control shRNA but not in HEK-MRP4 shRNA (Fig. 4*C*), indicating that the suppression of SNX27 increases the extrusion of [^{14}C]6MP by inducing MRP4 expression on the plasma membrane. HEK-control shRNA transfected with SNX27 siRNA extruded 1.7- and 1.6-fold more [^{14}C]6MP after 10 and 30 min of incubation, respectively, than did those with control siRNA.

The result of the efflux assay using [^{14}C]6MP was reflected in the sensitivity of these cells to 6MP and 6TG, a guanine analog

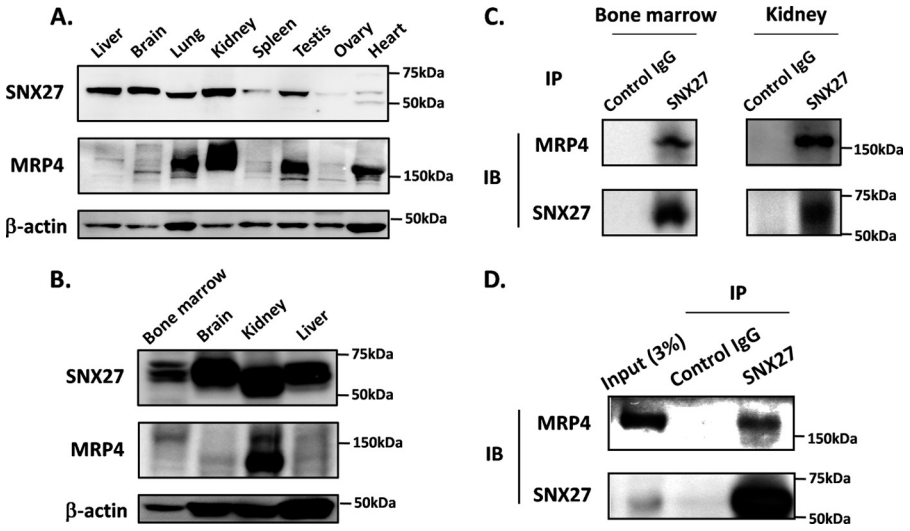

FIGURE 2. **Tissue distribution of SNX27 and its interaction with MRP4.** *A*, tissue distribution of SNX27 in humans. A commercially available human multiple-tissue blot was probed with antibodies against SNX27, MRP4, and β-actin. *B*, tissue distribution of SNX27 in mice. Homogenates prepared from mouse bone marrow, brain, kidney, and liver were subjected to Western blot analysis. *C* and *D*, interaction between endogenous MRP4 and SNX27 in mouse bone marrow and kidney (*C*) and HEK293 cells (*D*). SNX27 was immunoprecipitated (*IP*) from tissue homogenates of mouse bone marrow and kidney and lysates of HEK293 cells using anti-SNX27 antibody. Immunoprecipitated specimens were subjected to Western blot analysis (*IB*). *B–D*, representative result from three independent experiments.

of 6MP (Fig. 4, *D* and *E*, and Table 1). In HEK-control shRNA, the transfection of SNX27 siRNA increased the resistance to 6MP by 3.3-fold and resistance to 6TG by 2.5-fold. By contrast, in HEK-MRP4 shRNA, SNX27 suppression had no significant effect on 6MP- and 6TG-induced toxicity. Sensitivity to etoposide, which is not a substrate of MRP4, was not affected by the depletion of SNX27 and/or MRP4 (Fig. 4*F* and Table 1). These results indicate that SNX27 suppression confers resistance to both 6MP and 6TG by increasing MRP4 function, which increases the extrusion of their toxic metabolites. This finding was supported further by the similar expression level of HPRT1, which mediates the conversion of 6MP and 6TG to toxic metabolites, and of thiopurine methyltransferase, which methylates 6MP and reduces its toxicity, and the similar uptake ability of [^{14}C]6MP in HEK-MRP4 shRNA and HEK-control shRNA transfected with SNX27 siRNA or control siRNA (Fig. 4, *A* and *B*).

Subcellular Localization of SNX27—The subcellular localization of SNX27 was investigated using cell surface biotinylation and immunocytochemistry. Cell surface biotinylation showed the presence of SNX27 in the cell surface fraction, although the ratio of its amount in the cell surface fraction to that in input material was much lower than that of MRP4, a plasma membrane marker (Fig. 5*A*). EEA1 and hepatocyte growth factor-regulated tyrosine kinase substrate, which are both early endosome markers, were not observed in the cell surface fraction, indicating no contamination by the intracellular fraction. Because the lesser distribution of SNX27 in the cell surface fraction indicates a subcellular distribution other than in the plasma membrane, immunocytochemistry was applied to COS-1 cells, which are used widely in membrane sorting studies (29). SNX27 colocalized with EEA1 but not with LAMP-1, a lysosome marker (Fig. 5*B*), as reported previously (15). Alexa594 Tfn taken up into COS-1 cells colocalized with SNX27 as peripheral dotlike structures for up to 10 min after the start of its uptake but accumulated in the perinuclear regions and colocalized poorly with SNX27 30 min after uptake began (Fig. 5*C*). Given that, after internalization, Tfn is transferred initially to early endosomes and is then sorted to recycling endosomes, this indicates that SNX27 localized mainly in early endosomes but not in recycling endosomes. These findings were supported further by the colocalization of SNX27 with exogenously expressed AcGFP-Rab4 (Fig. 5*D*) and AcGFP-Rab5 (Fig. 5*E*), early endosome markers, but poorly with exogenously expressed AcGFP-Rab7 (Fig. 5*F*), a late endosome marker, and AcGFP-Rab11 (Fig. 5*G*), a recycling endosome marker. AcGFP-Rab4 and AcGFP-Rab5 did not colocalize with LAMP-1, suggesting that the merged immunosignals from SNX27 and AcGFP-Rab4 or AcGFP-Rab5 (Fig. 5, *D* and *E*) were derived from their colocalization and not from their coclustering (supplemental Fig. 1).

Involvement of SNX27 in MRP4 Internalization—To explore the involvement of SNX27 in intracellular sorting of MRP4 because of its endosomal and cell surface localization, we used cell surface biotinylation to investigate the degradation rate of MRP4 on the plasma membrane in HEK293 cells. These *in vitro* studies were conducted by depleting without overexpressing SNX27 because overexpression of SNXs can have secondary effects on intracellular trafficking by inducing tubulation of the endosomal network (30). Suppression of SNX27 by SNX27 siRNA transfection significantly delayed the degradation of cell surface-resident MRP4 (Fig. 6, *A* and *B*). The amounts of biotin-labeled MRP4 remaining after the 10- and 20-h incubations were about 2-fold higher in SNX27-depleted cells than in control cells (Fig. 6*B*). SNX27 suppression did not alter the degradation rate of the Na^+/K^+-ATPase α1 subunit on the plasma membrane (Fig. 6*A*).

Because MRP4 on the plasma membrane is thought to be degraded through the endosomal-lysosomal pathway after internalization (31), to investigate the mechanism by which

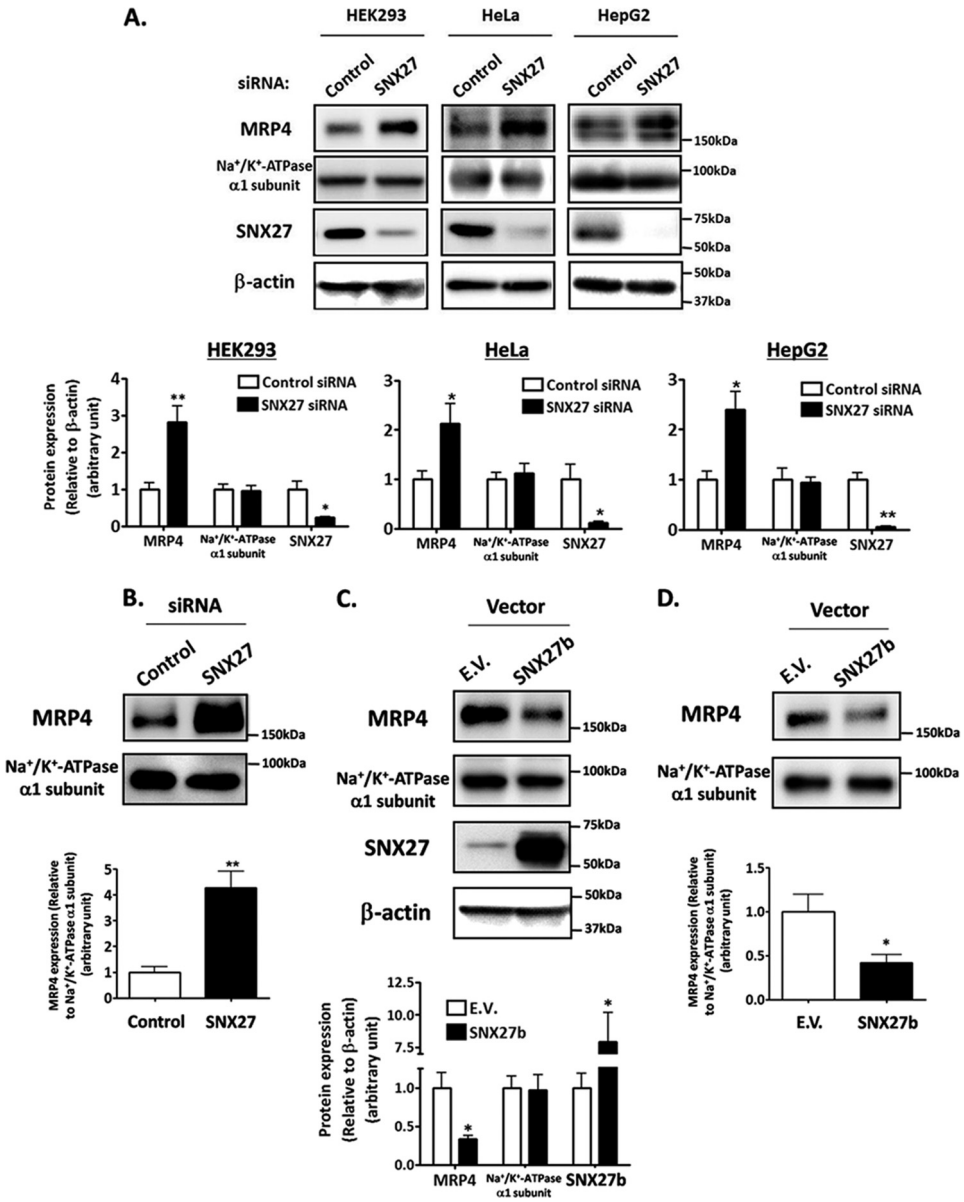

FIGURE 3. **Regulation of MRP4 expression by SNX27.** Depletion (*A* and *B*) and overexpression (*C* and *D*) of SNX27. HEK293 (*A–D*), HeLa (*A*), and HepG2 (*A*) cells were transfected with SNX27 siRNA or control siRNA (*A* and *B*) and pcDNA3.1(+)-SNX27 or empty vector (*E.V.*) (*C* and *D*). After 48 h of transfection, cell lysates were prepared (*A* and *C*), and cell surface biotinylation (*B* and *D*) was performed as described under "Experimental Procedures." *Top*, prepared specimens were subjected to Western blot analysis. A representative result from three independent experiments is shown. *Bottom*, Image Gauge software was used to quantify the ratios of band intensities of each protein to that of β-actin (*A* and *C*) or Na^+/K^+-ATPase α1 subunit (*B* and *D*). Each *bar* represents the mean ± S.E. (*error bars*) of three to four independent experiments. *, $p < 0.05$; **, $p < 0.01$.

SNX27 modulates the degradation of cell surface-resident MRP4 in detail, endocytosis and recycling rates of MRP4 were measured using cell surface biotinylation in HEK293 cells. The endocytosis assay showed that the internalization rate of MRP4 was significantly delayed by SNX27 siRNA transfection (Fig. 7, *A* and *B*). The amounts of internalized MRP4 after 2- and 5-min incubations were 2.1- and 3.2-fold lower, respectively, in SNX27 siRNA-transfected HEK293 cells than in cells with control siRNA (Fig. 7*B*). By contrast, recycling of MRP4 to the plasma membrane was not affected by SNX27 suppression (Fig. 7, *C* and *D*). SNX27 suppression had no effect on either endocytosis or recycling of the Na^+/K^+-ATPase α1 subunit (Fig. 7, *A* and *C*).

DISCUSSION

The current study was designed to examine the mechanism regulating the cell surface expression of MRP4, which is responsible for the distribution of drugs and endogenous compounds in various tissues, such as the bone marrow, kidney, and brain (5–7). In contrast to the characterization of the physiological function of MRP4, its posttranslational mechanism remains unclear.

The PDZ-bm mediates correct sorting and tethering of membrane proteins to specific subcellular locations through interactions with proteins containing the PDZ domain (8, 9). Therefore, we searched for proteins that interact with the PDZ-bm of MRP4, which is located at its C-terminal end, using GST pull-down assays

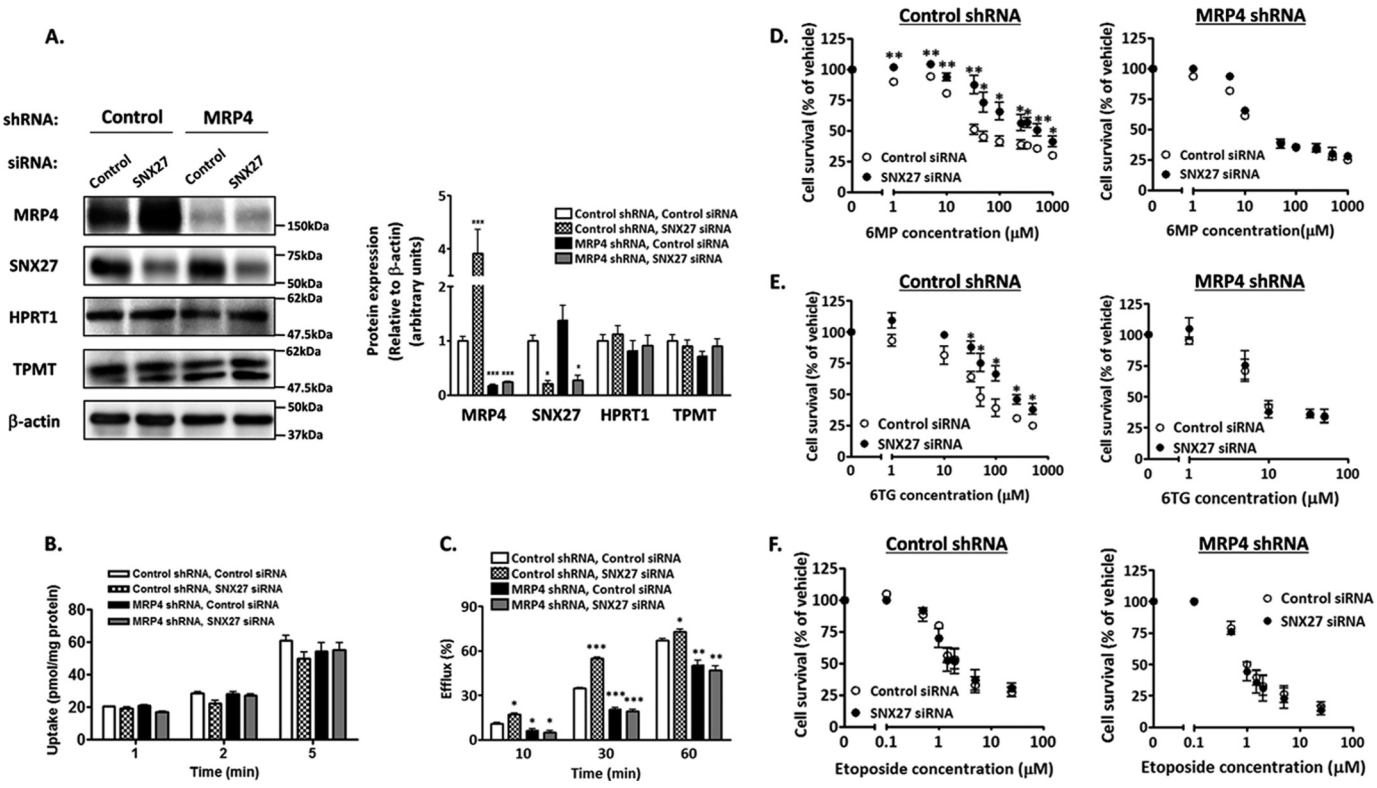

FIGURE 4. **Effect of SNX27 depletion on resistance to 6MP and 6TG.** HEK-MRP4 shRNA or HEK-control shRNA cells were transfected with SNX27 siRNA or control siRNA. After 24 h (*D–F*) or 48 h (*A–C*) of transfection, these cells were studied. *A*, expression of MRP4, SNX27, HPRT1, and thiopurine methyltransferase. *Left*, cell lysates were prepared and subjected to Western blot analysis. A representative result from four independent experiments is shown. *Right*, Image Gauge software was used to quantify the ratios of band intensities of each protein to that of β-actin. Each *bar* represents the mean ± S.E. (*error bars*) of four independent experiments. *, $p < 0.05$; ***, $p < 0.001$ compared with control siRNA-transfected HEK-control shRNA cells. *B*, time profiles of uptake of [^{14}C]6MP. Cells were incubated at 37 °C in KH buffer containing 5 μM [^{14}C]6MP, and its time-dependent uptake was determined. Each *bar* represents the mean ± S.E. of three independent experiments. *C*, time profiles of efflux of [^{14}C]6MP. Cells were incubated for 2 h as described in *B*, and the time-dependent efflux was determined. Each *bar* represents the mean ± S.E. of three independent experiments. ***, $p < 0.001$; **, $p < 0.01$; *, $p < 0.05$ compared with control siRNA-transfected HEK-control shRNA cells. *D–F*, sensitivity to 6MP, 6TG, and etoposide. Cells were incubated for 96 h in medium containing 6MP (*C*), 6TG (*D*), or etoposide (*E*) at the concentration indicated. Drug sensitivity was determined as described under "Experimental Procedures." Each point represents the mean ± S.E. from three independent experiments in triplicate. **, $p < 0.01$; *, $p < 0.05$.

TABLE 1

Growth inhibition of SNX27-depleted HEK293 cells by cytotoxic agents

The growth inhibition was measured as described under "Experimental Procedures." The IC_{50} values are the concentrations at which growth is inhibited by 50%. The IC_{50} values shown are the means ± S.E. of three independent experiments performed in triplicate. -Fold resistance (FR) is obtained by dividing the IC_{50} of SNX27 siRNA-transfected cells by that of control siRNA-transfected cells.

	Control shRNA			MRP4 shRNA		
Drug	Control siRNA IC_{50}	SNX27 siRNA IC_{50}	FR	Control siRNA IC_{50}	SNX27 siRNA IC_{50}	FR
	μM	μM	*-fold*	μM	μM	*-fold*
6MP	135 ± 47	446 ± 94	3.3[a]	29.5 ± 8.6	40.9 ± 17.9	1.3
6TG	84.2 ± 18.5	213 ± 39	2.5[a]	19.9 ± 9.6	15.8 ± 7.6	0.8
Etoposide	2.42 ± 0.60	2.40 ± 0.71	1.0	1.10 ± 0.20	0.94 ± 0.17	0.8

[a] Significant as determined by use of the nonparametric two-tailed Wilcoxon test ($p < 0.05$).

and subsequent MALDI-TOF MS analysis. We identified SNX27, a PDZ domain-containing protein, as the binding partner of MRP4. *In vitro* binding assays and a coimmunoprecipitation study confirmed that its interaction is via PDZ-PDZ interaction (Fig. 1, *B* and *C*) and is present in living cells (Fig. 2, *C* and *D*). Knockdown of SNX27 in HEK293 cells increased the cell surface expression of MRP4 and efflux of 6MP (Figs. 3*B* and 4, *C–E*, and Table 1). Further functional characterization of SNX27 in HEK293 cells using cell surface biotinylation showed that the suppression of this protein inhibits the degradation and internalization of cell surface-resident MRP4 but has no effect on its recycling to the plasma membrane (Figs. 6 and 7).

Given that MRP4 on the plasma membrane is degraded after internalization (31), the decrease in the degradation of cell surface-resident MRP4 by SNX27 depletion is probably caused by inhibition of its internalization from the plasma membrane. Our findings suggest that SNX27 can interact with MRP4 via PDZ-PDZ interaction and thereby regulate the cell surface expression and transport function of MRP4 by modulating its internalization process. This is the first report to evaluate MRP4 internalization directly and to show the molecules involved in its internalization process.

We used HEK293 and HeLa cells expressing FLAG-MRP4, FLAG-MRP4Δ4, MRP4, or MRP4Δ4 to try to confirm that the

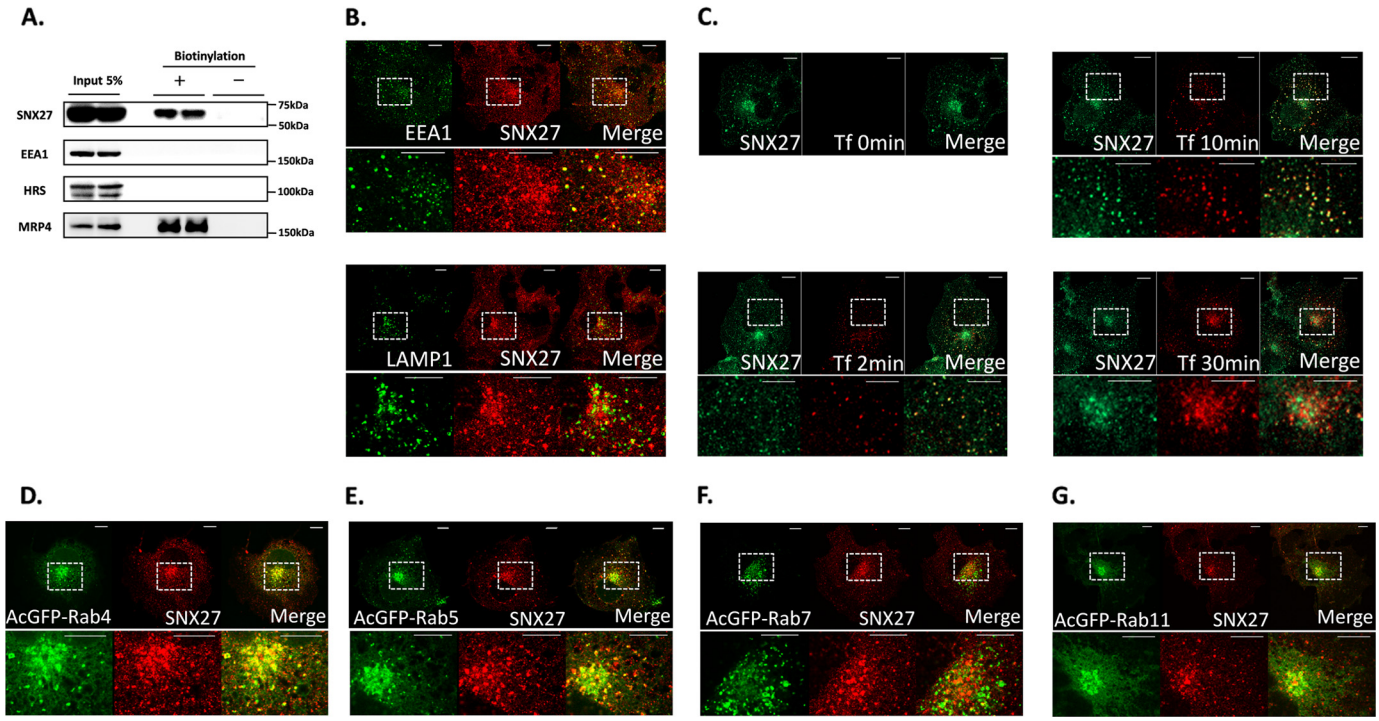

FIGURE 5. **Intracellular localization of SNX27.** *A*, cell surface biotinylation. HEK293 cells were biotinylated as described under "Experimental Procedures." The cell surface fraction and 5% of the input were analyzed by Western blot analysis. *B*, immunofluorescent colocalization study with organelle markers. COS-1 cells were fixed and stained with anti-SNX27 antibody and anti-EEA1 antibody or anti-LAMP1 antibody for confocal immunofluorescence microscopy as described under "Experimental Procedures." *C*, uptake of Alexa594 Tfn. COS-1 cells were incubated in DMEM containing Alexa594 Tfn (100 μg/ml) at 37 °C for the durations indicated, after which the medium was harvested, and the ligand remaining on the cell surface was released using an acid wash. The cells were then stained with anti-SNX27 antibody for confocal immunofluorescence microscopy as described under "Experimental Procedures." *D–G*, immunofluorescent colocalization study with Rab proteins. COS-1 cells transfected with pAcGFP-C1 containing Rab4 (*D*), Rab5 (*E*), Rab7 (*F*), or Rab11 (*G*) were stained with anti-SNX27 antibody for confocal immunofluorescence microscopy as described under "Experimental Procedures." The *lower images* in *B–G* are enlargements of the areas indicated by the *squares* in the *upper images* in *B–G*. *Yellow* in the *merged images* of *B–G* indicates colocalization. *Scale bar*, 10 μm (*B–G*). A representative result from three independent experiments is shown.

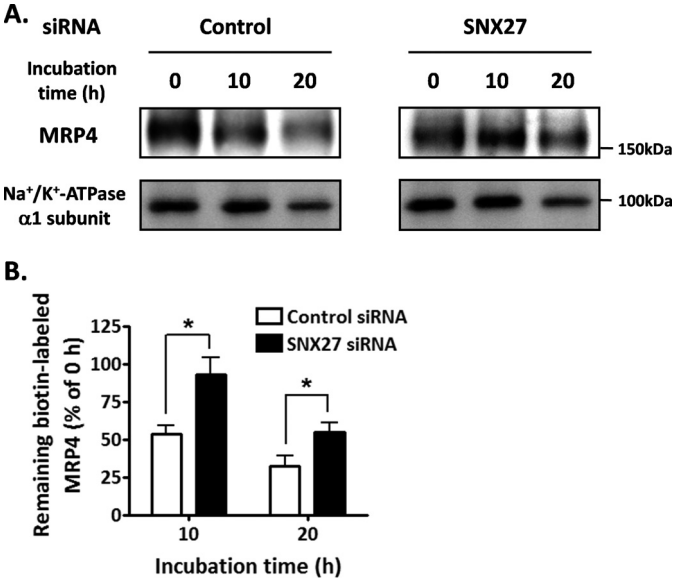

FIGURE 6. **Effect of SNX27 on the degradation rate of cell surface-resident MRP4.** *A*, HEK293 cells transfected with control siRNA or SNX27 siRNA were biotinylated and incubated at 37 °C for the times indicated, as described under "Experimental Procedures." The remaining biotin-labeled proteins isolated with streptavidin beads were subjected to Western blot analysis. *B*, quantification of the band indicating MRP4 in *A*. The signal intensity of the band was quantified using Image Gauge software and is expressed as a percentage of the MRP4 present at 0 h. Each *bar* represents the mean ± S.E. (*error bars*) of three independent experiments. *, $p < 0.05$.

effect of SNX27 on MRP4 is mediated through the PDZ-PDZ interaction. In contrast to endogenous MRP4, the expression of exogenously expressed MRP4 was positively regulated by SNX27, and the expression level of MRP4Δ4 was not affected by SNX27 expression (data not shown).

The colocalized dotlike structure of MRP4 with SNX27, suggesting the colocalization of both proteins in early endosomes and in vesicles directed to early endosomes, was hardly detectable in our immunocytochemical study using HeLa cells and COS-1 cells (data not shown); however, the lack of such a pattern in our immunocytochemical study does not contradict our current finding that SNX27 mediates MRP4 internalization. Given that only 4–5% of cell surface-resident MRP4 is internalized per minute (Fig. 7, *A* and *B*) and that most of the MRP4 internalized is recycled to the plasma membrane within 5 min (Fig. 7, *C* and *D*), it is conceivable that, at steady state, MRP4 localizes predominantly to the plasma membrane and to a much lesser extent in SNX27-positive vesicles. This hypothesis is supported further by the result of the coimmunoprecipitation assay, showing that the ratio of the amount of MRP4 to that of SNX27 was much smaller in the coimmunoprecipitates with SNX27 than that in the input specimen (Fig. 2*D*).

Hoque and Cole (31) used immunocytochemistry with monensin, an inhibitor of membrane protein recycling, to show that Na^+/H^+ exchanger regulatory factor isoform 1 (NHERF1), another PDZ domain-containing protein, may promote MRP4

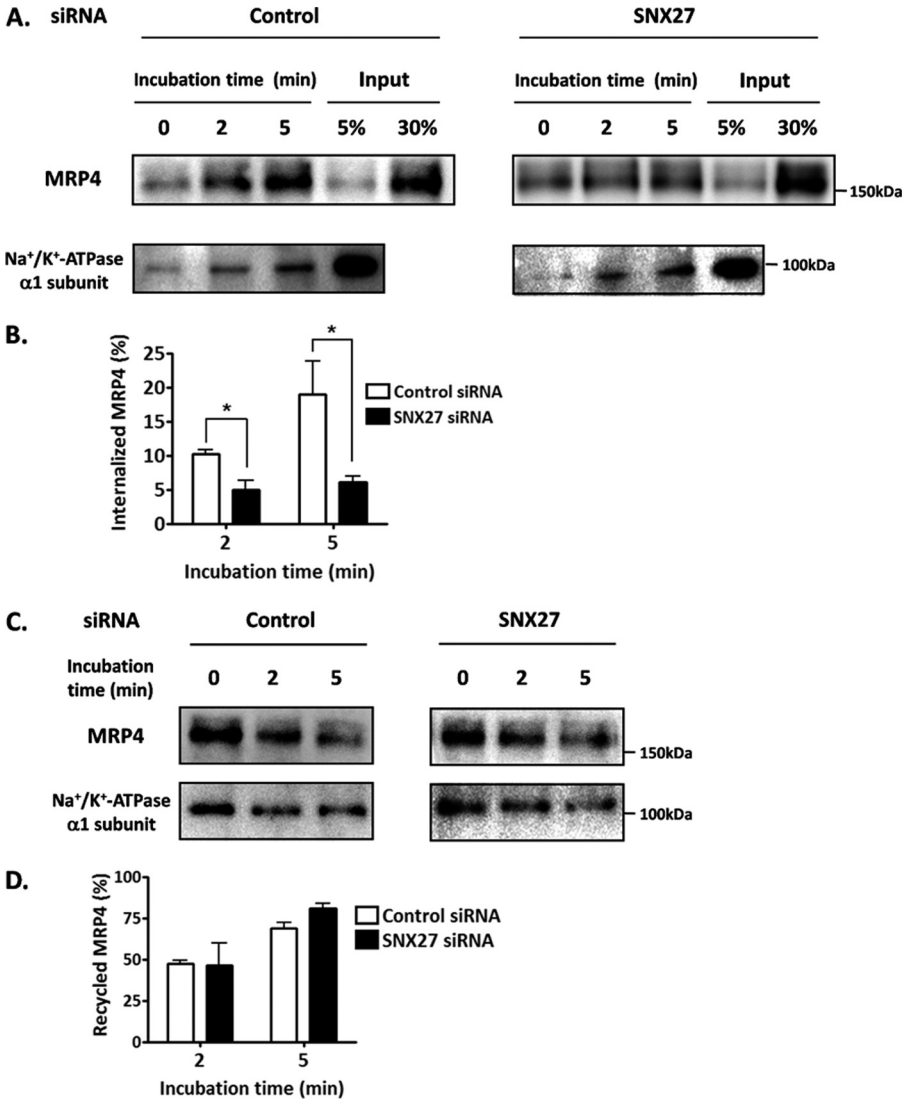

FIGURE 7. **Effect of SNX27 on endocytosis and recycling of MRP4.** After 48 h of control siRNA or SNX27 siRNA transfection, HEK293 cells were subjected to an endocytosis assay (*A* and *B*) or recycling assay (*C* and *D*) as described under "Experimental Procedures." *A* and *B*, measurement of the endocytosis of MRP4. *A*, the internalized sulfo-NHS-SS-biotin-labeled proteins were precipitated with streptavidin-agarose beads and subjected to Western blot analysis. *B*, quantification of the internalized MRP4 relative to the surface pool. Data were derived from the band corresponding to MRP4 in *A*. The signal intensity was quantified using Image Gauge software. Internalization at 0 min was normalized to 0%. Each *bar* represents the mean ± S.E. from three independent experiments. *, $p < 0.05$. *C* and *D*, measurement of the recycling of MRP4. *C*, the internalized sulfo-NHS-SS-biotin-labeled proteins remaining after incubation at 37 °C for the time indicated were precipitated with streptavidin-agarose beads and subjected to Western blot analysis. *D*, quantification of recycled MRP4 relative to the endocytosed pool. Data were derived from the band corresponding to MRP4 in *C*. The signal intensity was quantified using Image Gauge software. The recycling of MRP4 was calculated as described under "Experimental Procedures." Each *bar* represents the mean ± S.E. (*error bars*) from three independent experiments.

internalization. NHERF1 regulates the internalization of membrane proteins, but the influence of this adaptor protein varies depending on the proteins interacting with the PDZ-bm. In other words, the disruption of NHERF1 function inhibits the internalization of the parathyroid hormone receptor (32), whereas it promotes chemokine receptor CCR5, as is the case for MRP4 (33). NHERF1 increases the recruitment of arrestin-2 to CCR5 (33), which can facilitate the internalization of CCR5 by targeting it to clathrin-coated pits through the interaction between arrestin-2, the AP2 adaptor complex (AP2), and clathrin (34). At present, we do not know how SNX27 accelerates the internalization of MRP4. However, if the internalization of MRP4 is mediated by clathrin-mediated endocytosis involving NHERF1, arrestin, AP2, and clathrin, as occurs for CCR5, SNX27 may work on the cargo selection process and its subsequent recruitment to clathrin-coated pits through PDZ-PDZ interaction. This would confer high substrate selectivity to the clathrin-mediated endocytosis machinery. This hypothesis is supported by the results showing that the suppression of SNX27 expression had no effect on the internalization rate of the Na^+/K^+-ATPase α1 subunit (Fig. 7*A*) and the uptake of [^{125}I]Tfn,[4] both of which are mediated in an AP2- and clathrin-dependent manner (35, 36). These indicate that SNX27 is not implicated in the fundamental processes of clathrin-mediated endocytosis, such as the formation of a putative nucleation module on the plasma membrane where clathrin is recruited, clathrin coat assembly, and scission of clathrin-coated vesicles from the plasma

[4] H. Hayashi, S. Naoi, T. Nakagawa, T. Nishikawa, H. Fukuda, S. Imajoh-Ohmi, A. Kondo, K. Kubo, T. Yabuki, A. Hattori, M. Hirouchi, and Y. Sugiyama, unpublished data.

membrane (37). Given that the low density lipoprotein receptor appears to have cargo-specific adaptors, autosomal recessive hypercholesterolemia, and disabled homologue 2, which recruit low density lipoprotein receptor to AP2 (37), it is conceivable that SNX27 is an adaptor protein that specifically recruits the membrane proteins with the PDZ-bm to clathrin-coated pits.

SNX27 has been reported to interact with 5-$HT_{4(a)}$R, the cytohesin-associated scaffolding protein, diacylglycerol kinase ζ, β2AR, Kir3 channels, and NR2C via PDZ-PDZ interaction and to modulate intracellular sorting of these proteins (12–16, 38). The results of our study are consistent with the results of immunocytochemical analysis for 5-$HT_{4(a)}$R, Kir3 channels, and NR2C, showing that SNX27 targets these membrane proteins to early endosomes (12, 13, 15). However, our results are inconsistent with those for β2AR, which show that SNX27 promotes the trafficking of the β2AR from endosomes to the plasma membrane thorough its entry into retromer (14, 38). At present, we do not know why SNX27 had no effect on MRP4 recycling (Fig. 7, *C* and *D*) despite the predominant localization of the former protein in early endosomes and to a lesser extent in the cell surface in our experimental system (Fig. 5). One possible explanation is that different recycling pathways are used for MRP4 and the β2AR. β2AR uses the SNX27/retromer-mediated recycling pathway from EEA1-positive endosomes to the plasma membrane (38), whereas MRP4 can be recycled to the plasma membrane predominantly using other routes such as the Rab11-dependent recycling pathway. Unlike endogenous MRP4, the expression of exogenously expressed MRP4 was controlled positively by SNX27 (data not shown). This difference may reflect the localization of MRP4 to early endosomes, where SNX27 and β2AR, but not endogenous MRP4, are accessible because of saturation of the normal intracellular trafficking pathway of MRP4 by its high transient expression, facilitating the SNX27/retromer-mediated recycling of MRP4 to the plasma membrane and consequent increase in its cell surface expression.

In conclusion, our *in vitro* studies suggest that SNX27 associates physically with MRP4 through PDZ-PDZ interaction, which promotes the internalization of MRP4 and thereby negatively regulates its cell surface expression and transport function. MRP4 makes a vital contribution to the bodily distribution of xenobiotics and endogenous compounds through its cellular efflux abilities (6, 7). Therefore, impaired regulation of MRP4 and of other reported proteins that interact with SNX27 may be responsible for growth and survival defects in the SNX27 gene-deleted mice (12). Further studies on the physiological function of MRP4 would provide mechanistic insights into these phenotypes.

In addition to a role in the intracellular trafficking shown in this study, PDZ-PDZ interaction seems to be essential for the physiological function of MRP4 because MRP4 forms macromolecular complexes with CFTR at the apical membrane of gut epithelial cells, where these complexes are involved in the regulation of CFTR-mediated chloride currents (7). Future research to characterize further the proteins interacting with the PDZ-bm of MRP4 and their functions would advance our understanding of the posttranslational regulation of MRP4, including its intracellular trafficking and physiological function.

Acknowledgment—We thank Dr. Larissa Kogleck for advice on the manuscript.

REFERENCES

1. Kool, M., de Haas, M., Scheffer, G. L., Scheper, R. J., van Eijk, M. J., Juijn, J. A., Baas, F., and Borst, P. (1997) Analysis of expression of cMOAT (MRP2), MRP3, MRP4, and MRP5, homologues of the multidrug resistance-associated protein gene (MRP1), in human cancer cell lines. *Cancer Res.* **57,** 3537–3547
2. Borst, P., and Elferink, R. O. (2002) Mammalian ABC transporters in health and disease. *Annu. Rev. Biochem.* **71,** 537–592
3. Chen, Z. S., Lee, K., and Kruh, G. D. (2001) Transport of cyclic nucleotides and estradiol 17-β-D-glucuronide by multidrug resistance protein 4. Resistance to 6-mercaptopurine and 6-thioguanine. *J. Biol. Chem.* **276,** 33747–33754
4. Schuetz, J. D., Connelly, M. C., Sun, D., Paibir, S. G., Flynn, P. M., Srinivas, R. V., Kumar, A., and Fridland, A. (1999) MRP4. A previously unidentified factor in resistance to nucleoside-based antiviral drugs. *Nat. Med.* **5,** 1048–1051
5. Imaoka, T., Kusuhara, H., Adachi, M., Schuetz, J. D., Takeuchi, K., and Sugiyama, Y. (2007) Functional involvement of multidrug resistance-associated protein 4 (MRP4/ABCC4) in the renal elimination of the antiviral drugs adefovir and tenofovir. *Mol. Pharmacol.* **71,** 619–627
6. Krishnamurthy, P., Schwab, M., Takenaka, K., Nachagari, D., Morgan, J., Leslie, M., Du, W., Boyd, K., Cheok, M., Nakauchi, H., Marzolini, C., Kim, R. B., Poonkuzhali, B., Schuetz, E., Evans, W., Relling, M., and Schuetz, J. D. (2008) Transporter-mediated protection against thiopurine-induced hematopoietic toxicity. *Cancer Res.* **68,** 4983–4989
7. Li, C., Krishnamurthy, P. C., Penmatsa, H., Marrs, K. L., Wang, X. Q., Zaccolo, M., Jalink, K., Li, M., Nelson, D. J., Schuetz, J. D., and Naren, A. P. (2007) Spatiotemporal coupling of cAMP transporter to CFTR chloride channel function in the gut epithelia. *Cell* **131,** 940–951
8. Sugiura, T., Shimizu, T., Kijima, A., Minakata, S., and Kato, Y. (2011) PDZ adaptors. Their regulation of epithelial transporters and involvement in human diseases. *J. Pharm. Sci.* **100,** 3620–3635
9. Tonikian, R., Zhang, Y., Sazinsky, S. L., Currell, B., Yeh, J. H., Reva, B., Held, H. A., Appleton, B. A., Evangelista, M., Wu, Y., Xin, X., Chan, A. C., Seshagiri, S., Lasky, L. A., Sander, C., Boone, C., Bader, G. D., and Sidhu, S. S. (2008) A specificity map for the PDZ domain family. *PLoS Biol.* **6,** e239
10. Worby, C. A., and Dixon, J. E. (2002) Sorting out the cellular functions of sorting nexins. *Nat. Rev.* **3,** 919–931
11. Kajii, Y., Muraoka, S., Hiraoka, S., Fujiyama, K., Umino, A., and Nishikawa, T. (2003) A developmentally regulated and psychostimulant-inducible novel rat gene *mrt1* encoding PDZ-PX proteins isolated in the neocortex. *Mol. Psychiatry* **8,** 434–444
12. Cai, L., Loo, L. S., Atlashkin, V., Hanson, B. J., and Hong, W. (2011) Deficiency of sorting nexin 27 (SNX27) leads to growth retardation and elevated levels of *N*-methyl-D-aspartate receptor 2C (NR2C). *Mol. Cell. Biol.* **31,** 1734–1747
13. Joubert, L., Hanson, B., Barthet, G., Sebben, M., Claeysen, S., Hong, W., Marin, P., Dumuis, A., and Bockaert, J. (2004) New sorting nexin (SNX27) and NHERF specifically interact with the 5-HT4a receptor splice variant. Roles in receptor targeting. *J. Cell Sci.* **117,** 5367–5379
14. Lauffer, B. E., Melero, C., Temkin, P., Lei, C., Hong, W., Kortemme, T., and von Zastrow, M. (2010) SNX27 mediates PDZ-directed sorting from endosomes to the plasma membrane. *J. Cell Biol.* **190,** 565–574
15. Lunn, M. L., Nassirpour, R., Arrabit, C., Tan, J., McLeod, I., Arias, C. M., Sawchenko, P. E., Yates, J. R., 3rd, and Slesinger, P. A. (2007) A unique sorting nexin regulates trafficking of potassium channels via a PDZ domain interaction. *Nat. Neurosci.* **10,** 1249–1259
16. Rincón, E., Sáez de Guinoa, J., Gharbi, S. I., Sorzano, C. O., Carrasco, Y. R., and Mérida, I. (2011) Translocation dynamics of sorting nexin 27 in acti-

vated T cells. *J. Cell Sci.* **124,** 776–788
17. Valdes, J. L., Tang, J., McDermott, M. I., Kuo, J. C., Zimmerman, S. P., Wincovitch, S. M., Waterman, C. M., Milgram, S. L., and Playford, M. P. (2011) Sorting nexin 27 protein regulates trafficking of a p21-activated kinase (PAK) interacting exchange factor (β-Pix)-G protein-coupled receptor kinase interacting protein (GIT) complex via a PDZ domain interaction. *J. Biol. Chem.* **286,** 39403–39416
18. Mizuno, T., Hayashi, H., Naoi, S., and Sugiyama, Y. (2011) Ubiquitination is associated with lysosomal degradation of cell surface-resident ATP-binding cassette transporter A1 (ABCA1) through the endosomal sorting complex required for transport (ESCRT) pathway. *Hepatology* **54,** 631–643
19. Lowry, O. H., Rosebrough, N. J., Farr, A. L., and Randall, R. J. (1951) Protein measurement with the Folin phenol reagent. *J. Biol. Chem.* **193,** 265–275
20. Hayashi, H., and Sugiyama, Y. (2009) Short-chain ubiquitination is associated with the degradation rate of a cell-surface-resident bile salt export pump (BSEP/ABCB11). *Mol. Pharmacol.* **75,** 143–150
21. Miyagawa, M., Maeda, K., Aoyama, A., and Sugiyama, Y. (2009) The eighth and ninth transmembrane domains in organic anion transporting polypeptide 1B1 affect the transport kinetics of estrone-3-sulfate and estradiol-17β-D-glucuronide. *J. Pharmacol. Exp. Ther.* **329,** 551–557
22. Hayashi, H., Takada, T., Suzuki, H., Onuki, R., Hofmann, A. F., and Sugiyama, Y. (2005) Transport by vesicles of glycine- and taurine-conjugated bile salts and taurolithocholate 3-sulfate. A comparison of human BSEP with rat Bsep. *Biochim. Biophys. Acta* **1738,** 54–62
23. Hayashi, H., Takada, T., Suzuki, H., Akita, H., and Sugiyama, Y. (2005) Two common PFIC2 mutations are associated with the impaired membrane trafficking of BSEP/ABCB11. *Hepatology* **41,** 916–924
24. Hori, N., Hayashi, H., and Sugiyama, Y. (2011) Calpain-mediated cleavage negatively regulates the expression level of ABCG1. *Atherosclerosis* **215,** 383–391
25. Hayashi, H., and Sugiyama, Y. (2007) 4-Phenylbutyrate enhances the cell surface expression and the transport capacity of wild-type and mutated bile salt export pumps. *Hepatology* **45,** 1506–1516
26. Hayashi, H., Inamura, K., Aida, K., Naoi, S., Horikawa, R., Nagasaka, H., Takatani, T., Fukushima, T., Hattori, A., Yabuki, T., Horii, I., and Sugiyama, Y. (2012) AP2 mediates BSEP internalization and modulates its hepatocanalicular expression and transport function. *Hepatology* doi: 10.1002/hep.25591
27. Leggas, M., Adachi, M., Scheffer, G. L., Sun, D., Wielinga, P., Du, G., Mercer, K. E., Zhuang, Y., Panetta, J. C., Johnston, B., Scheper, R. J., Stewart, C. F., and Schuetz, J. D. (2004) Mrp4 confers resistance to topotecan and protects the brain from chemotherapy. *Mol. Cell. Biol.* **24,** 7612–7621
28. Wielinga, P. R., Reid, G., Challa, E. E., van der Heijden, I., van Deemter, L., de Haas, M., Mol, C., Kuil, A. J., Groeneveld, E., Schuetz, J. D., Brouwer, C., De Abreu, R. A., Wijnholds, J., Beijnen, J. H., and Borst, P. (2002) Thiopurine metabolism and identification of the thiopurine metabolites transported by MRP4 and MRP5 overexpressed in human embryonic kidney cells. *Mol. Pharmacol.* **62,** 1321–1331
29. Misaki, R., Nakagawa, T., Fukuda, M., Taniguchi, N., and Taguchi, T. (2007) Spatial segregation of degradation- and recycling-trafficking pathways in COS-1 cells. *Biochem. Biophys. Res. Commun.* **360,** 580–585
30. Carlton, J., Bujny, M., Rutherford, A., and Cullen, P. (2005) Sorting nexins. Unifying trends and new perspectives. *Traffic* **6,** 75–82
31. Hoque, M. T., and Cole, S. P. (2008) Down-regulation of Na^+/H^+ exchanger regulatory factor 1 increases expression and function of multidrug resistance protein 4. *Cancer Res.* **68,** 4802–4809
32. Sneddon, W. B., Syme, C. A., Bisello, A., Magyar, C. E., Rochdi, M. D., Parent, J. L., Weinman, E. J., Abou-Samra, A. B., and Friedman, P. A. (2003) Activation-independent parathyroid hormone receptor internalization is regulated by NHERF1 (EBP50). *J. Biol. Chem.* **278,** 43787–43796
33. Hammad, M. M., Kuang, Y. Q., Yan, R., Allen, H., and Dupre, D. J. (2010) Na^+/H^+ exchanger regulatory factor-1 is involved in chemokine receptor homodimer CCR5 internalization and signal transduction but does not affect CXCR4 homodimer or CXCR4-CCR5 heterodimer. *J. Biol. Chem.* **285,** 34653–34664
34. Moore, C. A., Milano, S. K., and Benovic, J. L. (2007) Regulation of receptor trafficking by GRKs and arrestins. *Annu. Rev. Physiol.* **69,** 451–482
35. Doné, S. C., Leibiger, I. B., Efendiev, R., Katz, A. I., Leibiger, B., Berggren, P. O., Pedemonte, C. H., and Bertorello, A. M. (2002) Tyrosine 537 within the Na^+,K^+-ATPase α-subunit is essential for AP-2 binding and clathrin-dependent endocytosis. *J. Biol. Chem.* **277,** 17108–17111
36. Motley, A., Bright, N. A., Seaman, M. N., and Robinson, M. S. (2003) Clathrin-mediated endocytosis in AP-2-depleted cells. *J. Cell Biol.* **162,** 909–918
37. McMahon, H. T., and Boucrot, E. (2011) Molecular mechanism and physiological functions of clathrin-mediated endocytosis. *Nat. Rev. Mol. Cell Biol.* **12,** 517–533
38. Temkin, P., Lauffer, B., Jäger, S., Cimermancic, P., Krogan, N. J., and von Zastrow, M. (2011) SNX27 mediates retromer tubule entry and endosome-to-plasma membrane trafficking of signaling receptors. *Nat. Cell Biol.* **13,** 715–721